HAL
open science

Lateral Distribution of the Radio Signal in Extensive Air Showers Measured with LOPES

W.D. Apel, J.C. Arteaga, T. Asch, A.F. Badea, L. Bähren, K. Bekk, M. Bertaina, P.L. Biermann, J. Blümer, H. Bozdog, et al.

To cite this version:

W.D. Apel, J.C. Arteaga, T. Asch, A.F. Badea, L. Bähren, et al.. Lateral Distribution of the Radio Signal in Extensive Air Showers Measured with LOPES. Astroparticle Physics, 2009, 32 (6), pp.294. 10.1016/j.astropartphys.2009.09.007 . hal-00510614

HAL Id: hal-00510614

https://hal.science/hal-00510614v1

Submitted on 20 Aug 2010

HAL is a multi-disciplinary open access archive for the deposit and dissemination of scientific research documents, whether they are published or not. The documents may come from teaching and research institutions in France or abroad, or from public or private research centers.

L'archive ouverte pluridisciplinaire **HAL**, est destinée au dépôt et à la diffusion de documents scientifiques de niveau recherche, publiés ou non, émanant des établissements d'enseignement et de recherche français ou étrangers, des laboratoires publics ou privés.

Accepted Manuscript

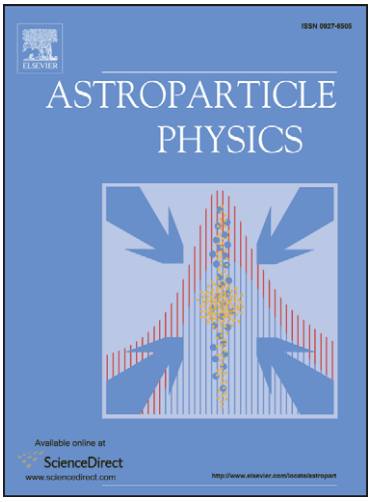

Lateral Distribution of the Radio Signal in Extensive Air Showers Measured with LOPES

W.D. Apel, J.C. Arteaga, T. Asch, A.F. Badea, L. Bähren, K. Bekk, M. Bertaina, P.L. Biermann, J. Blümer, H. Bozdog, I.M. Brancus, M. Brüggemann, P. Buchholz, S. Buitink, E. Cantoni, A. Chiavassa, F. Cossavella, K. Daumiller, V. de Souza, F. Di Pierro, P. Doll, R. Engel, H. Falcke, M. Finger, D. Fuhrmann, H. Gemmeke, P.L. Ghia, R. Glasstetter, C. Grupen, A. Haungs, D. Heck, J.R. Hörandel, A. Horneffer, T. Huege, P.G. Isar, K.-H. Kampert, D. Kang, D. Kickelbick, O. Krömer, J. Kuijpers, S. Lafebre, P. Łuczak, M. Ludwig, H.J. Mathes, H.J. Mayer, M. Melissas, B. Mitrica, C. Morello, G. Navarra, S. Nehls, A. Nigl, J. Oehlschläger, S. Over, N. Palmieri, M. Petcu, T. Pierog, J. Rautenberg, H. Rebel, M. Roth, A. Saftoiu, H. Schieler, A. Schmidt, F. Schröder, O. Sima, K. Singh, G. Toma, G.C. Trinchero, H. Ulrich, A. Weindl, J. Wochele, M. Wommer, J. Zabierowski, J.A. Zensus

PII: S0927-6505(09)00142-X
DOI: 10.1016/j.astropartphys.2009.09.007
Reference: ASTPHY 1435

To appear in: *Astroparticle Physics*

Received Date: 10 April 2009
Revised Date: 27 August 2009
Accepted Date: 23 September 2009

Please cite this article as: W.D. Apel, J.C. Arteaga, T. Asch, A.F. Badea, L. Bähren, K. Bekk, M. Bertaina, P.L. Biermann, J. Blümer, H. Bozdog, I.M. Brancus, M. Brüggemann, P. Buchholz, S. Buitink, E. Cantoni, A. Chiavassa, F. Cossavella, K. Daumiller, V. de Souza, F. Di Pierro, P. Doll, R. Engel, H. Falcke, M. Finger, D. Fuhrmann, H. Gemmeke, P.L. Ghia, R. Glasstetter, C. Grupen, A. Haungs, D. Heck, J.R. Hörandel, A. Horneffer, T. Huege, P.G. Isar, K.-H. Kampert, D. Kang, D. Kickelbick, O. Krömer, J. Kuijpers, S. Lafebre, P. Łuczak, M. Ludwig, H.J. Mathes, H.J. Mayer, M. Melissas, B. Mitrica, C. Morello, G. Navarra, S. Nehls, A. Nigl, J. Oehlschläger, S. Over, N. Palmieri, M. Petcu, T. Pierog, J. Rautenberg, H. Rebel, M. Roth, A. Saftoiu, H. Schieler, A. Schmidt, F. Schröder, O. Sima, K. Singh, G. Toma, G.C. Trinchero, H. Ulrich, A. Weindl, J. Wochele, M. Wommer, J. Zabierowski, J.A. Zensus, Lateral Distribution of the Radio Signal in Extensive Air Showers Measured with LOPES, *Astroparticle Physics* (2009), doi: 10.1016/j.astropartphys.2009.09.007

ACCEPTED MANUSCRIPT

This is a PDF file of an unedited manuscript that has been accepted for publication. As a service to our customers we are providing this early version of the manuscript. The manuscript will undergo copyediting, typesetting, and review of the resulting proof before it is published in its final form. Please note that during the production process errors may be discovered which could affect the content, and all legal disclaimers that apply to the journal pertain.

ACCEPTED MANUSCRIPT

ACCEPTED MANUSCRIPT

Lateral Distribution of the Radio Signal in Extensive Air Showers Measured with LOPES

W.D. Apel [a], J.C. Arteaga [b,2], T. Asch [c], A.F. Badea [a], L. Bähren [d], K. Bekk [a], M. Bertaina [e], P.L. Biermann [f], J. Blümer [a,b], H. Bozdog [a], I.M. Brancus [g], M. Brüggemann [h], P. Buchholz [h], S. Buitink [d], E. Cantoni [e,i], A. Chiavassa [e], F. Cossavella [b], K. Daumiller [a], V. de Souza [b,3], F. Di Pierro [e], P. Doll [a], R. Engel [a], H. Falcke [d,j], M. Finger [a], D. Fuhrmann [k], H. Gemmeke [c], P.L. Ghia [i], R. Glasstetter [k], C. Grupen [h], A. Haungs [a], D. Heck [a], J.R. Hörandel [d], A. Horneffer [d], T. Huege [a], P.G. Isar [a], K.-H. Kampert [k], D. Kang [b], D. Kickelbick [h], O. Krömer [c], J. Kuijpers [d], S. Lafebre [d], P. Łuczak [ℓ], M. Ludwig [b], H.J. Mathes [a], H.J. Mayer [a], M. Melissas [b], B. Mitrica [g], C. Morello [i], G. Navarra [e], S. Nehls [a,1], A. Nigl [d], J. Oehlschläger [a], S. Over [h], N. Palmieri [b], M. Petcu [g], T. Pierog [a], J. Rautenberg [k], H. Rebel [a], M. Roth [a], A. Saftoiu [g], H. Schieler [a], A. Schmidt [c], F. Schröder [a], O. Sima [m], K. Singh [d,4], G. Toma [g], G.C. Trinchero [i], H. Ulrich [a], A. Weindl [a], J. Wochele [a], M. Wommer [a], J. Zabierowski [ℓ], J.A. Zensus [f]

[a] *Institut für Kernphysik, Forschungszentrum Karlsruhe, Germany*

[b] *Institut für Experimentelle Kernphysik, Universität Karlsruhe, Germany*

[c] *IPE, Forschungszentrum Karlsruhe, Germany*

[d] *Department of Astrophysics, Radboud University Nijmegen, The Netherlands*

[e] *Dipartimento di Fisica Generale dell' Universita Torino, Italy*

[f] *Max-Planck-Institut für Radioastronomie Bonn, Germany*

[g] *National Institute of Physics and Nuclear Engineering, Bucharest, Romania*

[h] *Fachbereich Physik, Universität Siegen, Germany*

[i] *Istituto di Fisica dello Spazio Interplanetario, INAF Torino, Italy*

[j] *ASTRON, Dwingeloo, The Netherlands*

[k] *Fachbereich Physik, Universität Wuppertal, Germany*

[ℓ] *Soltan Institute for Nuclear Studies, Lodz, Poland*

ACCEPTED MANUSCRIPT

[m] *Department of Physics, University of Bucharest, Bucharest, Romania*

Abstract

The antenna array LOPES is set up at the location of the KASCADE-Grande extensive air shower experiment in Karlsruhe, Germany and aims to measure and investigate radio pulses from Extensive Air Showers. The coincident measurements allow us to reconstruct the electric field strength at observation level in dependence of general EAS parameters. In the present work, the lateral distribution of the radio signal in air showers is studied in detail. It is found that the lateral distributions of the electric field strengths in individual EAS can be described by an exponential function. For about 20% of the events a flattening towards the shower axis is observed, preferentially for showers with large inclination angle. The estimated scale parameters R_0, describing the slope of the lateral profiles range between 100 and 200 m. No evidence for a direct correlation of R_0 with shower parameters like azimuth angle, geomagnetic angle, or primary energy can be found. This indicates that the lateral profile is an intrinsic property of the radio emission during the shower development which makes the radio detection technique suitable for large scale applications.

1 Introduction

The traditional method to study extensive air showers (EAS), which are generated by high-energy cosmic rays entering the Earth's atmosphere, is to measure the secondary particles with sufficiently large particle detector arrays. In general, these measurements provide only immediate information on the status of the air shower cascade at the particular observation level. This hampers the determination of the properties of the primary inducing the EAS as compared to methods like the observation of Cherenkov and fluorescence light, which also provide information on the longitudinal EAS development, thus providing a more reliable access to the information of interest [1].

In order to reduce the statistical and systematic uncertainties of the detection and reconstruction of EAS, especially with respect to the detection of cosmic particles of highest energies, measuring the radio emission during the shower development is being discusses as a new detection technique. The radio waves

[1] corresponding author, *E-mail address:* nehls@ik.fzk.de
[2] now at: Universidad Michoacana, Morelia, Mexico
[3] now at: Universidade São Paulo, Instituto de Fisica de São Carlos, Brasil
[4] now at: KVI, University of Groningen, The Netherlands

ACCEPTED MANUSCRIPT

can be recorded day and night, and provide a bolometric measure of the electromagnetic shower component. Due to technical restrictions in past times, the radio emission accompanying cosmic ray air showers was a somewhat neglected feature in the past. However, the study of this EAS component has experienced a revival by recent activities, in particular by the LOPES project [2,3]. LOPES as pathfinder for large scale radio detection for the LOFAR project [4] and the Pierre Auger Observatory [5] investigates the correlations of radio data with shower parameters reconstructed by the extensive air shower experiment KASCADE-Grande [6]. Hence, LOPES, which is designed as a digital radio interferometer using large bandwidth and fast data processing, profits from the reconstructed air shower observables of KASCADE-Grande.

The main goal of the investigations in the frame of LOPES is the understanding of the shower radio emission in the primary energy range of 10^{16} eV to 10^{18} eV. Of particular interest is the investigation of the correlation of the measured field strength with main shower parameters. These are the orientation of the shower axis (azimuth angle, zenith angle, and the geomagnetic angle, i.e. the angle between shower axis and geomagnetic field), the position of the observer relative to the shower axis, and the energy and mass (electron and muon number) of the primary particle. Another goal of LOPES (LOPES^{STAR}) is the optimization of the hardware (antenna design and electronics) for a large scale application of the detection technique including a self-trigger mechanism for a stand-alone radio operation [7].

In the present study we investigate in detail the lateral profile of the radio signal as measured by LOPES. Due to a precise amplitude calibration of each individual antenna and the event information from KASCADE-Grande, this is possible on an event-by-event basis with high accuracy. Such investigations are of great interest as the lateral shape defines the optimum grid size for a radio antenna array in a stand-alone mode. Of particular interest is the scale parameter which describes the amount of the signal decrease with distance from the shower axis and the dependence of that parameter on characteristics of the primary particle. In addition, knowing the lateral extension in detail will contribute to the understanding of the emission mechanism of the radio signal as simulations have shown [8], that the lateral shape can be related to important physical quantities such as the primary energy or the mass of the primary.

ACCEPTED MANUSCRIPT

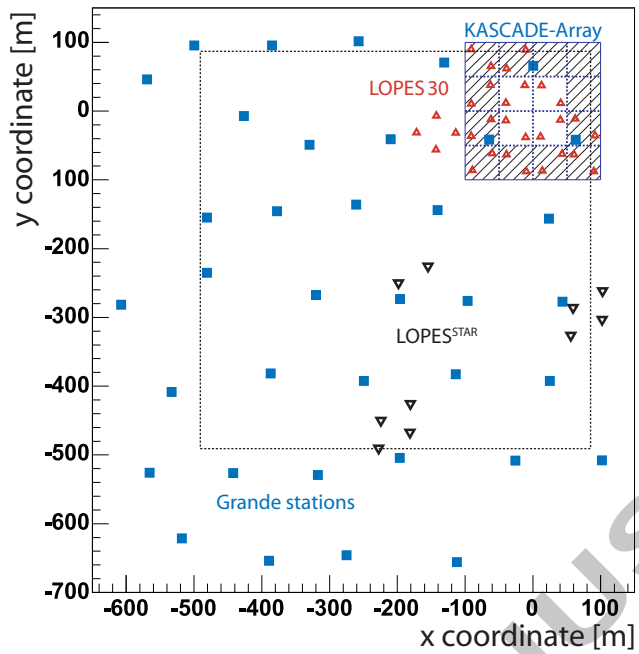

Fig. 1. Sketch of the KASCADE-Grande – LOPES experiments: The squared 16 clusters (12 with muon counters) of the KASCADE field array, the distribution of the 37 stations of the Grande array, the location of the 30 LOPES radio antennas, and the positions of the 10 newly developed LOPES^{STAR} antennas. The dotted line shows the area used for the present analysis.

2 The LOPES Experiment

2.1 Experimental Setup

LOPES has been set-up as prototype station of the LOFAR project to verify the detection of radio emission from air showers. The basic idea is to use an array of relatively simple, quasi omni-directional dipole antennas. The signals are digitized and sent to a central computer in which the registered waves from the individual antennas are superimposed (software interferometer). With LOPES it is possible to buffer the received data stream for a certain period of time. After a detection of a transient phenomenon like an air shower, a beam in the desired direction can be formed in retrospect. To demonstrate the capability to measure air showers with such antennas, LOPES is situated at the air shower experiment KASCADE-Grande. KASCADE-Grande is an extension of the multi-detector setup KASCADE [9] (KArlsruhe Shower Core and Array DEtector) built in Germany, measuring the charged particles of air showers in the primary energy range of 10^{14} eV to 10^{18} eV with high precision due to the detection of the electromagnetic and the muonic shower component separately with independent detector systems. Hence, on the one hand LOPES profits from the reconstructed air shower observables of KASCADE-Grande, but on

ACCEPTED MANUSCRIPT

the other hand, since radio emission arises from different phases of the EAS development, LOPES is intended to provide complementary information to the particle detector arrays of KASCADE-Grande.

The antenna configuration of LOPES has changed several times in order to study different aspects of the radio emission. With the extension of the antenna field from 10 to 30 east-west orientated antennas in 2005 (LOPES30), the baseline and the low noise amplifier (LNA) performance at the antennas improved. In the configuration used in the analysis described here, LOPES operated 30 short dipole radio antennas. The LOPES antennas, positioned within or close to the original KASCADE array (fig. 1), operate in the frequency range of $40 - 80\,\mathrm{MHz}$ and are aligned in east-west direction, i.e. they are mainly sensitive to the linear east-west polarized component of the radiation. This layout was in particular chosen to provide the possibility for a detailed investigation of the lateral extension of the radio signal as it has a maximum baseline of approximately 260 m. The read-out window for each antenna is 0.8 ms wide centered around the trigger received from the KASCADE array; the sampling rate is 80 MHz. The logical condition to trigger the LOPES data readout is a high multiplicity of fired particle detector stations of the KASCADE array. This corresponds to primary energies above $\approx 10^{16}$ eV; which are detected with a rate of ≈ 2 per minute.

2.2 Data Calibration

Each single LOPES radio antenna has an absolute amplitude calibration at its location inside the KASCADE-Array (end-to-end calibration), performed using a commercial reference antenna [10] of known electric field strength at a certain distance. The power to be received from the source in calibration mode is compared with the power recorded in the LOPES electronics. The calibration procedure leads to frequency dependent amplification factors representing the complete system behavior (antenna, cables, electronics) in the environment of the KASCADE-Grande experiment. These correction factors are applied to the measured signal strengths resulting in electric field strengths which are used for further analysis. The systematic uncertainty of the calibration method ($\mathrm{sys}_{\mathrm{calib}} = 20.5\ \%$) is estimated from repeated measurement campaigns for individual antennas under all kinds of conditions. This uncertainty also includes, e.g., environmental effects, like those caused by different weather conditions over the two years of calibration campaigns. In particular, the antenna gain simulation contributes with an error of $\approx 10\%$ to the given total uncertainty [10].

The delay calibration of the system consists basically of two parts. First, the delay for each electronic channel is periodically verified with laboratory

ACCEPTED MANUSCRIPT

measurements of individual components and solar burst measurements of the complete signal chain. This delay was found to be almost stable over the operation time of LOPES. Second, a fine tuned correction of these delay times by a phase calibration is performed in order to catch short-time fluctuations in the trigger signal distribution and the data read-out. The delay calibration is always performed in reference to one antenna and the absolute time is connected to the data using the time stamps of KASCADE-Grande events. LOPES is operating three independent sub-stations with front-end electronics and requires the trigger from KASCADE-Grande in each station. By that, a jitter due to long transmitting intra-station cables is introduced. On basis of a known mono-frequent reference source with constant phase relation these disturbances are corrected. For the data sample used in this analysis, a TV-transmitter visible in the measured frequency range is used for the phase calibration [3].

2.3 Pulse Height Calculations

The LOPES data processing includes several steps. First, the relative instrumental delays are corrected using the known TV-transmitter. Next, the gain corrections, digital filtering, and corrections of the trigger delays based on the known shower direction (from KASCADE-Grande) are applied and noisy antennas are flagged. These steps include the application of the gain and phase calibration correction factors and also a correction for the azimuth and zenith dependence of the antenna gain.

The first step of the beam forming procedure [3] is the application of geometrical shifts of the data by the time difference of the pulse coming from the given direction to reach the position of the corresponding antenna. These shifts take into account the curvature of the electro-magnetic shower front (as free parameter to be fitted) and are done by multiplying a phase gradient in the frequency domain before transforming the data back to the time domain. To form the beam, the data from each pair of antennas are multiplied time-bin by time-bin, the resulting values are averaged, and then the square root is taken while preserving the sign: $cc(t) = \pm\sqrt{\left|\frac{1}{N_\mathrm{P}}\sum_{i=1}^{N-1}\sum_{j>i}^{N} s_i(t)s_j(t)\right|}$. From the number of unique pairs of antennas $N_\mathrm{P} = (N-1)N/2$ the normalization is determined. The coherence of the single antenna signals systematically influences the height and sign of this quantity, henceforth called the cc-beam [3]. In other words, the cc-beam is sensitive to and reflects the coherence of the radio pulse. The quantification of the radio parameters is done by fitting the smoothed (over three time-samples block averaged $\equiv 1/\Delta\nu$) cc-beam pulse, as shown in figure 2. In first approximation the shape of the resulting pulse can be fitted by a Gaussian giving a robust value for the peak strength, which is defined as the height of this Gaussian. The error of the fit results gives also a

ACCEPTED MANUSCRIPT

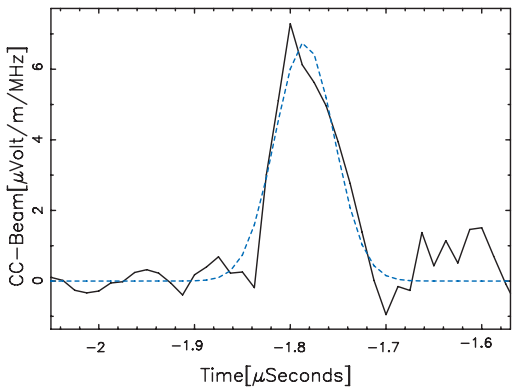

Fig. 2. The calculated cc-beam for an EAS is fit with a Gaussian function after block-averaging with a window of 37.5 ns. The height [μV/m/MHz] and the center in time [μs] of the fit are used as parameters for the radio analysis.

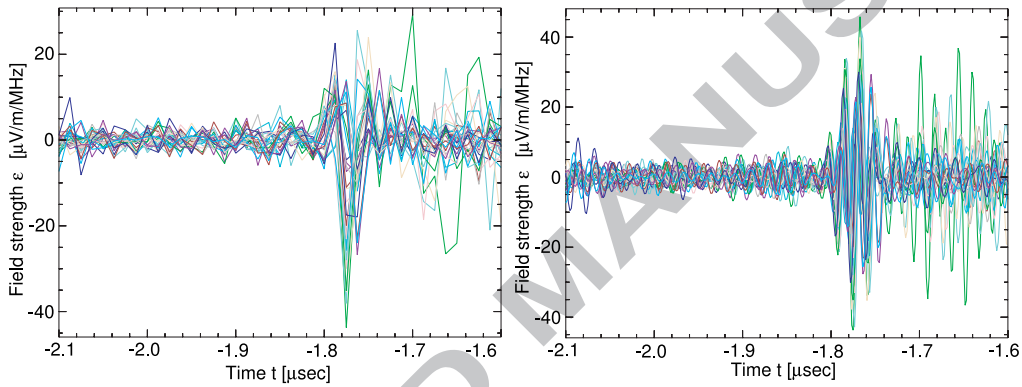

Fig. 3. Left: The sampled data with 12.5 ns spacing of the digitization with 80 MHz, in the second Nyquist domain. Right: The up-sampled signal shape between 40 MHz and 80 MHz.

first estimate of the uncertainty of this parameter. The finally obtained value ϵ_{cc}, which is the measured amplitude divided by the effective bandwidth, has usually been used for LOPES analyses.

While the cc-beam is an averaged property of the measured shower from all antennas, the present studies require the investigation of the field strength at individual antennas. The sampling of the data is done in the second Nyquist domain but a reconstruction of the original 40–80 MHz signal shape is needed to estimate the field strength per antenna. Therefore, an up-sampling of the data on a single antenna basis is performed (by the zero-padding method [5]) resulting in a band-limited interpolation in the time domain [11] to reconstruct

[5] Zero-padding is a method to extend a time series or a spectrum. Zeros are added in one domain and after Fourier transformation an interpolated series is obtained in the other domain. For the radio data the zero-padding is applied in the frequency domain and gives a band limited interpolation in the time domain. The up-sampling of a data set with N samples leads to a new data set with M samples. The up-sampling rate is given by $M/N = 2^n$, with $n = 0, 1, 2, \ldots$.

ACCEPTED MANUSCRIPT

the original signal form between the sampled data points with 12.5 ns spacing. The method can be applied, because all needed information after sampling in the second Nyquist domain is contained in the stored data [12]. An example how the method reconstructs the original signal shape is shown in figure 3, where an up-sampling with $n = 3$ is used.

After applying the zero-padding to the LOPES data, the radio signals can be used to reconstruct the electric field strength in each individual antenna. The Gaussian fit to the cc-beam defines the center of a time window with 45 nanoseconds width [6]. Within this time window, in the up-sampled data of each individual antenna the maximum absolute field strength is searched. This maximum value is used as the measured electric field strength ϵ per antenna and event. The window width is chosen to exclude the RFI appearing soon after the radio pulse signal. The RFI is caused by high currents in the particle detector cables during the penetration of the EAS. The systematic uncertainty of ϵ is estimated to 19%, stemming mainly from the calibration procedure.

As a further source of uncertainty, the contribution of the background to the signal is taken into account. To evaluate this noise, the mean of the absolute electric field strength from a defined time window (520 ns width ending 300 ns before the observed radio pulse) is calculated, where a typical value is in the order of 15-20% of the peak value of $|\epsilon|$ (see fig. 3). As one does not know if the noise is constructively or destructively interfering with the signal, the value of the noise level is not subtracted from ϵ, but added to the systematic uncertainty of the field strength.

2.4 Event Selection

The data set taken in the period from 16 November 2005 until 8 December 2006 is used for the analysis presented here, where for the whole period the 30 LOPES antennas have been orientated in east-west direction. The data taking was interrupted in Summer 2006. During a thunderstorm on 27th of July an over-voltage in the trigger distribution system occurred, breaking the trigger electronics. The whole antenna field was back in data acquisition in September 2006. Shorter malfunctions of individual antennas are handled by flagging them and not using them in the analysis. In the relevant period, KASCADE generated 966,000 triggers that were sent to the LOPES DAQ-system. Roughly 10% of them could not be recorded due to the 1.5 s long dead-time for the read-out of the radio data from the memory boards. The general

[6] For technical reasons the cc-beam calculation could not be used on the up-sampled data at the time of this analysis. This is not affecting the results of the present study, as the cc-beam is used only for the selection of the events and the definition of the time window.

ACCEPTED MANUSCRIPT

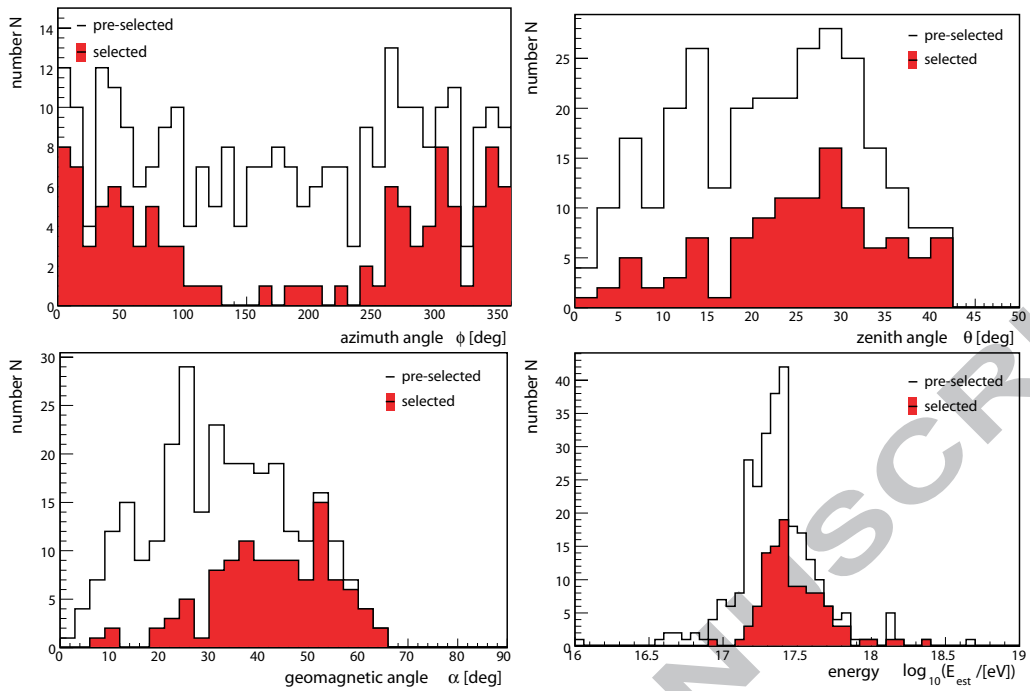

Fig. 4. Distribution of the azimuth angle ($0 \equiv$ North, $90 \equiv$ East), zenith angle, the geomagnetic angle, and the estimated primary energy E_{est} for all events selected by KASCADE-Grande parameters (pre-selected) and for the events with clear radio signals further considered in the analysis.

event reconstruction was performed for the remaining 860,000 events. Only a small fraction of this large amount of data shows radio signals significantly above the background due to the high RFI at the KASCADE-Grande site [13]. Only the highest energy EAS can give promising radio signals well above the noise needed for the investigation of lateral distributions in individual events. To select those, several cuts are applied: Firstly, the position of the shower axis has to be inside KASCADE-Grande, but not too far away from the antennas. Therefore, a square area of about 0.3 km^2 is used (see fig. 1). Secondly, the shower parameters are properly reconstructed from the KASCADE-Grande data, and the shower energy exceeds $3-5 \cdot 10^{16}$ eV based on cuts at the total electron and muon number of the shower.

The number of events selected by these cuts is $N = 296$. Twelve events have been found above a zenith angle of 44°, and are not used due to a generally more uncertain KASCADE-Grande reconstruction for inclined events. The radio data of the selected events are first analyzed with the procedures described above in order to find events with significant radio signals above the background. The criteria for such events are a successful cc-beam fit (which is fulfilled for nearly all selected high-energy events except a few arriving directly from South) and a radio signal higher than the noise per individual, not flagged, up-sampled antenna in a 45 ns window around the center of the cc-beam pulse. These requirements result in a total number of 110 events.

ACCEPTED MANUSCRIPT

The geometrical layout of the 30 antenna array and the applied selection area define the mean distance of the shower axis to the antennas ($70 - 250\,\mathrm{m}$; larger distances are suppressed due to the requirement on a clearly detected radio signal in all antennas) and the maximum baseline in individual events. A coverage of $100 - 300\,\mathrm{m}$ of the lateral distribution is obtained depending on the location of the shower core (see fig. 1).

In figure 4, the 110 radio events are compared to the original 284 events selected by KASCADE-Grande observables, only in their general air shower parameters. The azimuth angles of all pre-selected events are almost uniformly distributed over the whole angular range. An azimuth angle of 180° corresponds to showers arriving from the South. For this direction the relative angle to the direction of the geomagnetic field (geomagnetic angle) is smaller than for showers coming from the North [7]. If the magnetic field lines are nearly parallel to the shower axis, the radio emission is expected to be generally much weaker and its polarization more directed towards the north-south axis [2,14]. Therefore, as we measure only the east-west polarized component of the radio signal, no showers arriving from South fulfill the strict requirements to enter the further analysis. As an aside, this fact is a strong indication for a geomagnetic dependence of the radio emission. The zenith angle distribution has a mean of 22°, which is in agreement with the distribution of zenith angles of all KASCADE-Grande reconstructed events. Above 35° zenith angle the fraction of radio events increases, as inclined showers have larger geomagnetic angles and therefore a larger signal-to-noise ratio compared to nearly vertical showers, being closer to the orientation of the Earth's magnetic field. In addition, inclined showers show a larger footprint on ground and the noise from the particle detectors is smaller. At a fixed location the distribution of the geomagnetic angle incorporates the azimuth and zenith angle distributions, as both angles have to be used to calculate the geomagnetic angle α.

The primary energy E_{est} is roughly estimated from the KASCADE reconstructed muon and electron numbers with an accuracy of $\log(E_{\mathrm{est}}/\mathrm{GeV}) \approx \pm 0.15$. The arrival direction resolution of KASCADE-Grande is better than one degree for these high-energy events. The obtained distribution of the estimated primary energy is also shown in figure 4, where the majority of the selected EAS have energies above $10^{17.2}\,\mathrm{eV}$.

[7] The orientation of the magnetic field at the LOPES location is given by $\theta_b = 25°$ and $\phi_b = 180°$. Showers from the South are almost parallel to the magnetic field and the resulting Lorentz force is very small.

ACCEPTED MANUSCRIPT

3 Lateral Distributions of the Radio Signal in EAS

3.1 Reconstruction

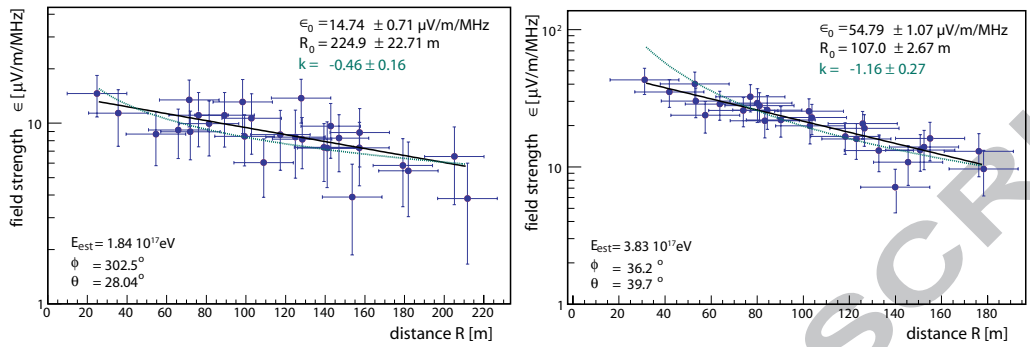

Fig. 5. Lateral distributions reconstructed from single antenna signals, shown for two individual showers. The full and dashed lines show the result of an exponential and power law fit, respectively. The left panel shows the same event as used for figure 2 and the right panel as used for figure 3.

To investigate the lateral behavior of the radio signal in individual events an exponential function $\epsilon = \epsilon_0 \cdot \exp\left(-R/R_0\right)$ is used to describe the measured field strengths. The fit contains two free parameters, where the scale parameter R_0 describes the lateral slope and ϵ_0 the extrapolated field strength at the shower axis at observation level. The number of antennas used for the determination of the two fit parameters can change from event to event, because an antenna can be flagged if the signal is disturbed by too high noise or by a technical malfunction at the time of the event. For comparisons, the signals of each event is also described by the best fitting power law $\epsilon = \epsilon_p \cdot R^k$.

Examples of events including the resulting lateral field strength functions are shown in figure 5. The error bars of the individual values in x- and y-direction are derived from the field strength and distance estimation, respectively. The uncertainty of the field strengths is calculated in a conservative way and includes the uncertainty of the antenna calibration and a value appointed to the maximum contribution of the noise. To avoid implicit assumptions on the lateral behavior of the field strength, we consider each antenna data as an individual measurement. But by that, the errors in x-direction and the uncertainties from the antenna calibration are not independent from other data points in an individual event and the significance of the fit results will be slightly reduced. The displayed showers are typical for almost all investigated events of which the distribution could be apparently described by an exponential function. The power law function in most cases tends to overestimate the lateral behavior close to the shower core, which also lead to a slightly worse quality of the fits (χ^2/ndf). Therefore, in the further analysis mainly the results of fits with the exponential function is considered.

ACCEPTED MANUSCRIPT

3.2 Unusual Lateral Profiles

For roughly 20% of the events lateral distributions have been found which do not show a clear exponential or power law fall-off. Four of these special distributions are shown in figure 6.

The shower displayed top left shows apparently a behavior as others do, but there appears a flattening for small distances. Maybe, it could be considered that a fit of two functions with a break at $\approx 140\,\mathrm{m}$ would better describe the lateral profile. There are about 15 events that exhibit such a slope change to a flatter lateral distribution close to the shower axis. The shower displayed top right shows another example of such events, but here the flattening occurs at $\approx 100\,\mathrm{m}$.

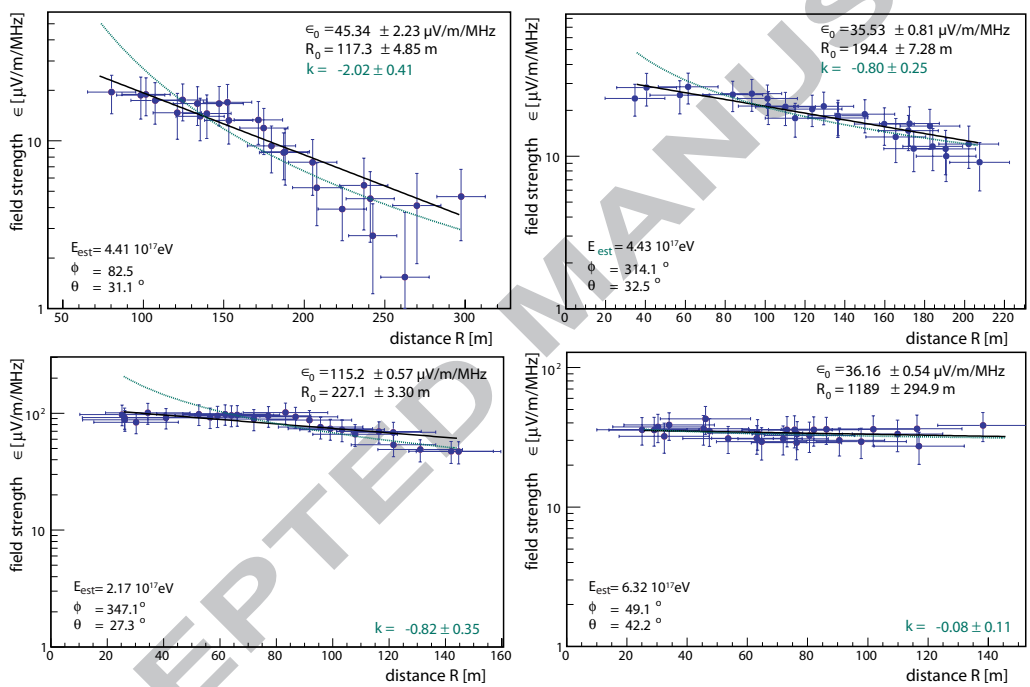

Fig. 6. Same as Fig. 5, but for four lateral distributions with unusual shapes. Discussion see text.

Also, for the shower in the bottom left panel a slope change at a distance of about 90 m can be seen. In addition, this particular shower shows a lateral distribution that is very flat for the distance range up to 90 m.

The even more extreme case of a flat lateral distribution is shown in the bottom right panel of figure 6. Over the whole distance range that could be measured, there is almost no fall-off in field strength.

It should be remarked that at field strengths above $5\,\mu\mathrm{V/m/MHz}$ the ambient noise background cannot affect the measurement and for none of the investi-

ACCEPTED MANUSCRIPT

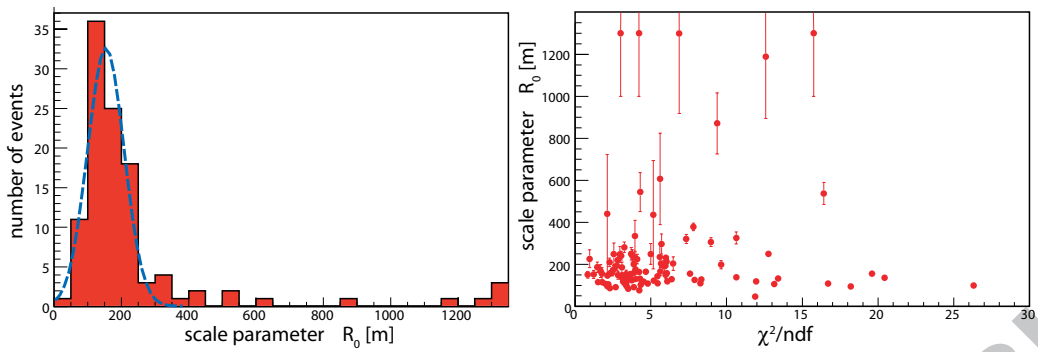

Fig. 7. Distribution of the scale parameter R_0. There are four events set to $R_0 = 1300\,\mathrm{m}$ whose actual R_0 values are higher, i.e. these are very flat events. The dashed line displays a Gaussian fit to the distribution in the range $R_0 = 0 - 300\,\mathrm{m}$ resulting in $\bar{R}_0 = 157\,\mathrm{m}$ with a width of 54 m. The right panel shows the goodness-of-fit parameter in correlation with the obtained R_0.

gated events a saturation of an antenna occurred. Also no known instrumental or selection effects can explain such shapes, and no strange environmental conditions like a thunderstorm appeared during these events. However, for a statistically reliable analysis, too few of such flat lateral profiles have been measured so far.

3.3 The Scale Parameter R_0

The scale parameter R_0 describes the slope of the lateral distribution. Most of the showers have a scale parameter smaller than 250 m (figure 7). There are some showers with extremely large scale parameter, $R_0 > 1300\,\mathrm{m}$, that are set in the plots to $R_0 = 1300\,\mathrm{m}$. The distribution peaks at a scale parameter of $R_0 \approx 125\,\mathrm{m}$, but due to the $\approx 10\%$ of very flat showers the median value is $R_0 = 155\,\mathrm{m}$ for the complete sample. Fitting a Gaussian function to the distribution of the scale parameter in the range of $0 - 300\,\mathrm{m}$, i.e. neglecting the flat events, a mean value of $\bar{R}_0 = 157\,\mathrm{m}$ with a width of 54 m is obtained (figure 7).

As the uncertainty in signal strength is estimated in a conservative way and by that the errors of individual measures are not independent, the fit quality in terms of χ^2/ndf is reduced. The right panel of figure 7 displays the individual χ^2/ndf in relation to the obtained scale parameter R_0, where no correlation is found, not even for the unusual flat profiles.

For a more detailed study of the lateral distributions the properties of the scale parameter and possible correlations with EAS parameters have been investigated. In case of the LOPES experiment this can be done easily, as the shower parameters are obtained from the KASCADE-Grande measurements. For ex-

ACCEPTED MANUSCRIPT

ample, the shower arrival direction may play a role for the obtained shape of the lateral distribution. In order to test this, the scale parameter is correlated with the geomagnetic angle α (using an $(1 - \cos\alpha)$-functional dependence[8]), the azimuth angle ϕ, and the zenith angle θ (figure 8). A correlation is found neither between the geomagnetic angle and R_0 nor between the azimuth angle and R_0.

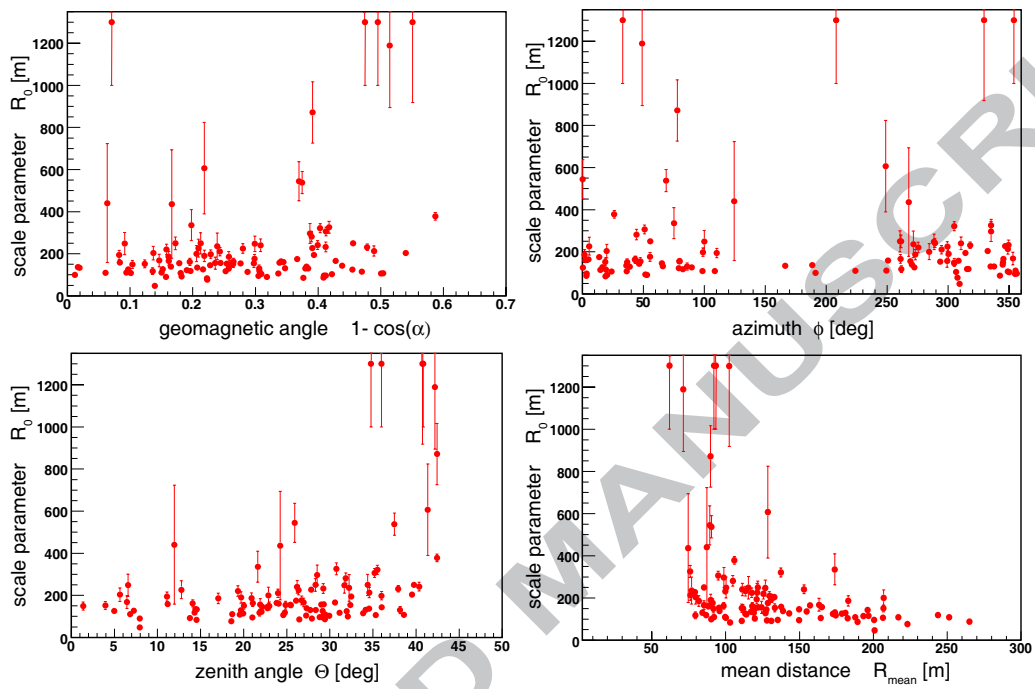

Fig. 8. Relations of the scale parameter R_0 with geomagnetic, azimuth, and zenith angle of the showers as well as with the mean distance of the antennas to the shower axes. The error bars show the uncertainty obtained by the fit with the exponential function.

The situation is different when the scale parameter is correlated with the zenith angle of the incoming primary cosmic ray (lower left panel of figure 8). Here a tendency towards larger values of the scale parameter is seen for inclined events. Expectations from simulations [16] that very inclined showers in general exhibit a larger scale parameter cannot be directly proven, as the cut for the zenith angle larger than 44° inhibits any further conclusions at the moment.

A clearer feature is seen, when the scale parameter is analyzed with respect to the corresponding mean distance to the shower axis of all antennas participating in an individual event (figure 8, bottom right panel). It is obvious that

[8] Using the cc-beam it was found that this functional form describes best the correlation of the field strength measured with LOPES with the geomagnetic field; at least for the east-west polarization component [15].

ACCEPTED MANUSCRIPT

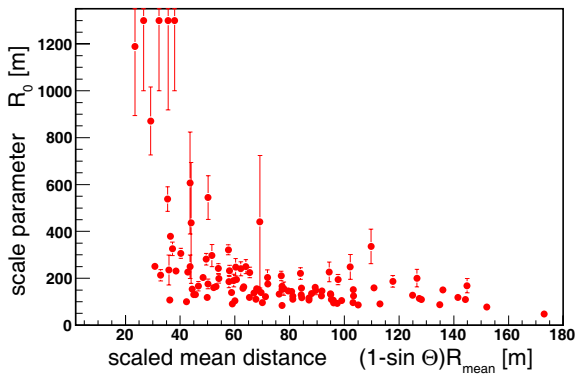

Fig. 9. Relation of the scale parameter R_0 with the mean distance of the antennas to the shower axis scaled with the zenith angle of the axis.

for a fraction of the events the lateral profile gets flatter when we measure closer to the shower center. In particular, all the very flat events have a mean distance below $R_0 \approx 80\,\mathrm{m}$. This is connected with the fact that we see showers which flatten towards the shower core, as discussed in the previous section.

An even more pronounced dependence of the scale parameter of flat events is seen when the mean distance is combined with the zenith angle information in the form $R'_{\mathrm{mean}} = (1 - \sin\Theta) \cdot R_{\mathrm{mean}}$. Figure 9 shows clearly that the probability of a flattening increases when the shower is inclined and when measured closer to the shower axis. Cutting events with $R'_{\mathrm{mean}} < 50\,\mathrm{m}$ and fitting again a Gaussian function to the distribution of the scale parameter in the range of $0 - 300\,\mathrm{m}$, the mean value and width decrease to $\bar{R}_0 = 149\,\mathrm{m}$ and $\sigma = 50\,\mathrm{m}$, respectively. But as not all events with small R'_{mean} show a flattening the reason is still unclear and further investigations with larger statistics are required.

In addition, a comparison of the scale parameter with the estimated primary energy (figure 10, left panel) has been performed, where no correlation could be observed. This is also the case (not shown here) when the correlation of R_0 with the lateral scale parameter[9] of the particle component of the EAS is investigated.

3.4 The Absolute Field Strength ϵ_0

The second parameter from the fitting procedure ϵ_0 represents the field strength at the shower axis. It is obtained by extrapolating the measured lateral profile to the shower axis.

[9] The so-called 'age' of the extensive air shower, which is reconstructed by using the particle density measurements of KASCADE-Grande.

ACCEPTED MANUSCRIPT

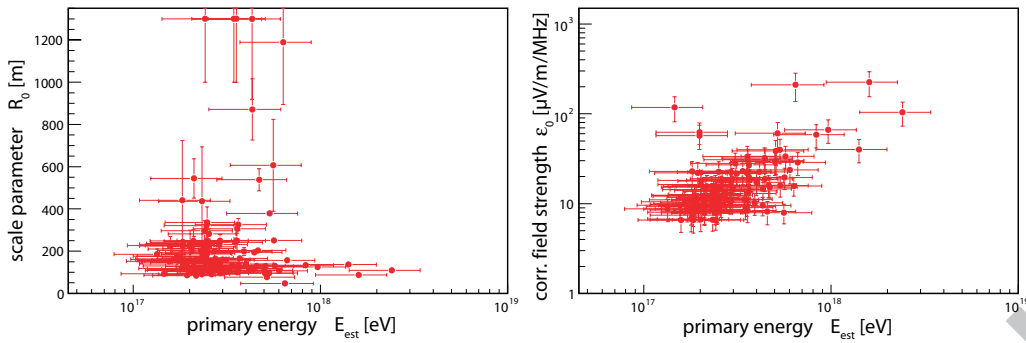

Fig. 10. The scale parameter R_0 (left panel) and the field strength at the shower center ϵ_0 (right panel) as a function of the estimated primary energy E_{est}. ϵ_0 is the result of a fit of the lateral distribution of single events corrected for the geomagnetic angle.

For the investigated events the fit of the field strength ϵ_0 yields values as expected from earlier investigations [15]. Figure 10, right panel, shows the relation of ϵ_0 versus the estimated primary energy E_{est}, where ϵ_0 is corrected for the geomagnetic angle with a (1-cos α)-dependence. The uncertainty of the estimated primary energy, as well as the systematic uncertainty in the amplitude calibration is taken into account. A clear dependence of ϵ_0 with the primary energy is visible following a power law $\epsilon_0 \propto E^{\kappa}$ with the index κ close to 1. This is expected if there is a coherent emission of the radio signal during the shower development. The absolute scale of the radio field strength as well as the extent and source of fluctuations are still under investigation and will be subject of a forthcoming paper.

3.5 Discussion

The lateral distributions of the electric field strength measured in individual events are described by exponential functions resulting in two parameters per EAS which are subject of further investigations. For most of the events the lateral distribution of the measured field strengths can also be described by a power law, though these fits tend to overestimate the signal strengths closer to the shower axis. The choice of the exponential dependence is also driven by simulation studies which predict an exponential fall-off of the lateral distribution [14]. Results from LOPES data analysis investigating the dependence of the cc-beam values with mean distance of the antennas to the shower axis [15] have also shown an exponential behavior, as well as early investigations leading to the parametrization of Allan 1971 [17], and results from the CODALEMA experiment [18].

The scale parameter R_0 obtained from the fits has a relatively narrow peak at $R_0 \approx 125$ m and a long tail with partially very large scale parameters. No

ACCEPTED MANUSCRIPT

direct dependence of R_0 on the geomagnetic angle, the primary energy and the azimuth angle could be found, which indicates that the shape of the lateral distribution is an intrinsic property of the radio emission in extensive air showers. Inclusion of the tail of the distribution in figure 7 leads to a mean value that agrees with the cc-beam based scale parameter in the parameterization results of LOPES [15], whereas the exclusion of the tail yields a scale parameter that agrees with the parameterization of earlier data, e.g. $R_0 \approx 110\,\mathrm{m}$ by Allan [17]. One should have in mind that these earlier measurements compiled by Allan in ref. [17] were performed in narrow bandwidths, and the dependence of the lateral distribution on frequency is still an open issue. The CODALEMA experiment has measured a few individual events with scale parameters in the order of around 200 m [18] for the absolute signal measured in both polarization directions.

Roughly 10% of the investigated showers show very flat lateral distributions with scale parameters $R_0 > 300\,\mathrm{m}$ (examples shown in figure 6). It was found that these showers are preferably arriving with a larger inclination and have their core closer to the LOPES antennas, i.e. the mean distance of the antennas to the shower axis is relatively small. In approximately another 10% of the measured events we recognize a lateral distribution with a flattening towards the shower center, where the fit to the distribution reveals only a slight increase of the scale parameter R_0. Combining these two observations, the very flat showers are probably events where we only measure the flat part close to the axis. The observation of a slight increase of the average R_0 with zenith angle can serve as a confirmation that for inclined showers the enlarged footprint on ground might enhance the effect. It is not expected that an exponential or a power law will fit the lateral distribution of radio signals perfectly, because both lead to a discontinuity at the shower axis. Therefore a modification for small distances from the shower axis is to be expected. However, it has to be mentioned that the flattening is observed only in a small fraction of the measured events and these events are not distinguishable from the others. For the majority, a clear exponential behavior of the lateral distribution of the radio signal is observed. Instrumental, background or environmental (man-made or weather) effects can be excluded as the cause for the flattening of the radio profiles. Hence, these experimental clues are remarkable and require further investigations with higher statistics. Interesting is the fact, that also the CODALEMA experiment reported about a few events with such a flat lateral behavior close to the shower center [19].

A thorough understanding of the emission process is needed to understand the experimental findings. Besides the exponential lateral behavior predicted by the geo-synchrotron model [8], there are results from simulations which describe the lateral slope by a power law [20] and earlier calculations indicating a change of slope toward the shower axis [21]. No theoretical approach investigated so far, however, predicts slope parameters in the order of $500 - 1000\,\mathrm{m}$

ACCEPTED MANUSCRIPT

in any range of lateral distance.

Case studies of special lateral distributions are presently limited in statistics and demand a much larger data set. However, the observed flattening of the lateral distribution of the radio signal to the shower center is an unexpected feature, in particular as it is only observed for a fraction of the events. Detailed information about the corresponding air shower is required to understand the measured lateral profiles. This corroborates the unique quality of the coincide measurements of LOPES with KASCADE-Grande. Also the role of possible polarization effects and the effect of the chosen observing frequency window on the radio lateral distribution have to be considered.

The correlation of the estimated field strength at the shower axis (fig. 10) with the primary energy is a measure of the expected coherence of the radio emission in EAS. Due to the high detection threshold for the radio emission from EAS and the limit in the energy range for the KASCADE-Grande experiment most of the showers in this work are in a very narrow range of the primary energy. In LOPES radio data parameterizations [15] the power law index resulted to $\kappa = 0.95 \pm 0.04$. Also from simulations a relation is expected that can be described with an index κ for a range between 1 and 0.75 [16] changing with the depth of the particle number maximum $X_{\max}$ as a function of primary energy. Hence, the obtained correlation supports the expectation of a scaling of the field strength ϵ_0 with primary energy and therefore a coherent emission.

The measured scale parameter of minimum $R_0 = 100\,\mathrm{m}$ at an energy of around $10^{17}\,\mathrm{eV}$ can be used to perform a rough estimate of the needed grid size for a radio antenna array measuring EAS at higher energies, i.e. planned in the frame of the Pierre Auger Observatory [22]. Assuming the exponential behavior with $R_0 = 100\,\mathrm{m}$ and the linear energy dependence of the signal, the distance between two antennas may be increased to up to 230 m to measure an equal field strength when increasing the primary energy by a factor of ten.

4 Conclusions and Outlook

The described studies on lateral distributions of the radio signal in air showers are based on coincidence measurements of the LOPES radio antenna array and the air shower experiment KASCADE-Grande. This is a unique combination of two different detection techniques for EAS investigations. Furthermore, the obtained data of both experiments are well calibrated and can therefore be used to compare the properties of the radio emission with EAS parameters in detail. Such investigations aim to fully understand the radio emission in extensive air showers for primary energies below $10^{18}\,\mathrm{eV}$. In the frame of this work a calibrated data set of showers has been analyzed to study the lateral

ACCEPTED MANUSCRIPT

distribution of the radio emission in individual air showers.

The applied analysis method uses up-sampled signals from individual antennas to derive the electric field strength per unit bandwidth ϵ (40-80 MHz and east-west polarization cmponent, only). With the help of the reconstructed shower parameters from KASCADE-Grande the lateral distribution of the radio signal in EAS for individual events is obtained. Here, the uncertainty of the amplitude calibration and an antenna-by-antenna event-by-event background calculation enters into the uncertainty of the determined field strength ϵ. The uncertainty of the reconstructed geometry of the shower contributes to the uncertainty for the lateral distance R of each antenna. For 110 showers which have a large enough radio signal in all antennas the lateral shape of the signal as well as correlations with global shower parameters, like direction and energy, were studied.

Exponential as well as power law functions were applied to the measured profiles, where the first one slightly better describes the data. The exponential function has two free parameters, the field strength ϵ_0 at the shower axis, and the scale parameter R_0. The scale parameter R_0 is a quantity that describes the slope of the lateral profile. The scale parameter distribution shows a peak value of $R_0 \approx 125$ m and has a tail with very flat lateral distributions. Excluding the flat events a mean value of $\bar{R}_0 \approx 150$ m with a width of $\sigma = 50$ m was obtained. No direct evidence for a dependence on the shower parameters azimuth angle, geomagnetic angle, and primary energy could be found. This indicates that the lateral profile is an intrinsic property of the radio emission and the shower development. Comparing the obtained scale parameter with published values of earlier experiments, a good agreement has been found. Studying the lateral distributions in individual events, approximately 20% of the studied showers show a very flat lateral distribution or exhibit a flattening towards the shower center. Preferably, such showers arrive under larger zenith angle and axes are close to the antennas. But, there are too few such showers measured to derive any significant correlation with specific shower parameters. However, the result is an indication that there might be (at least for a part of the showers) additional, not yet understood effects of the radio emission during the shower development. In the near future, besides higher statistics delivered by LOPES, the LOFAR project with its hundreds of antennas will provide detailed information (including polarization effects) on the lateral distribution of the radio signal in EAS.

The present analysis concentrates on experimental findings, only, but for the understanding of the radio emission observed in EAS a comparison with detailed Monte-Carlo simulations on an event-to-event basis will be very important. This will be possible soon because of the performed amplitude calibration of LOPES and the estimate of the field strength at individual antennas. Due to a new simulation strategy, using more realistic air shower models derived

ACCEPTED MANUSCRIPT

from per-shower CORSIKA [23] simulations including radio emission simulations with REAS2 [14] and a simulation of the antenna response, detailed comparisons between LOPES measured events and simulations can be performed.

The future goal of the radio detection technique lies in a large scale application with hundreds of antennas. The quadratic dependence of the received radio power on primary energy and the comparatively (with respect to the electromagnetic component of EAS) large lateral scale parameter will make radio detection a cost effective method for measuring the longitudinal development of air showers of the highest energy cosmic rays.

Acknowledgements

LOPES has been supported by the German Federal Ministry of Education and Research. The KASCADE-Grande experiment is supported by the German Federal Ministry of Education and Research, the MIUR and INAF of Italy, the Polish Ministry of Science and Higher Education and the Romanian Ministry of Education and Research.

References

[1] A. Haungs, H. Rebel, M. Roth, Rep. Prog. Phys. **66**, 1145 (2003).

[2] H. Falcke et al. - LOPES Collaboration, Nature **435**, 313 (2005).

[3] A. Horneffer et al. - LOPES Collaboration, Int. Journ. Mod. Phys. A **21** Suppl., 168 (2006).

[4] H.R. Butcher, Proc. SPIE **5489**, 537 (2004).

[5] J. Abraham et al. - Pierre Auger Collaboration, NIM A **523**, 50 (2004).

[6] G. Navarra et al. - KASCADE-Grande Collaboration, NIM A **518**, 207 (2004).

[7] T. Asch et al. - LOPES Collaboration, Proc. of 30th ICRC, Merida, Mexico **5**, 1081 (2008).

[8] T. Huege, R. Ulrich, and R. Engel, Astrop. Phys. **30**, 96 (2008).

[9] T. Antoni et al. - KASCADE Collaboration, NIM A **513**, 429 (2003).

[10] S. Nehls et al., NIM A **589**, 350 (2008).

[11] S. Nehls, FZKA report **7440**, Forschungszentrum Karlsruhe (2008).

ACCEPTED MANUSCRIPT

[12] O. Krömer, FZKA report **7396**, Forschungszentrum Karlsruhe (2008), in German.

[13] W.D. Apel et al. - LOPES Collaboration, Astrop. Phys. **26**, 332 (2006).

[14] T. Huege, R. Engel, and R. Ulrich, Astrop. Phys. **27**, 392 (2007).

[15] A. Horneffer et al. - LOPES Collaboration, Proc. of 30th ICRC, Merida, Mexico, **4**, 83 (2007).

[16] T. Huege and H. Falcke, Astrop. Phys. **24**, 116 (2005).

[17] H.R. Allan, Prog. in Element. Part. Cos. Ray Phys. **10**, 171 (1971).

[18] D. Ardouin et al. - CODALEMA Collaboration, Astrop. Phys. **26**, 341 (2006).

[19] P. Lautridou et al. - CODALEMA Collaboration, Proc. ARENA 2008, NIM A doi:10.1016/j.nima.2009.03.164

[20] O. Scholten, K. Werner, F. Rusydi, Astrop. Phys. **29**, 94 (2008).

[21] T. Huege and H. Falcke, Astron. Astrophys. **412**, 19 (2003).

[22] A.M. van den Berg - Pierre Auger Collaboration, Proc. of 31th ICRC, Lodz, Poland, #icrc0232 (2009).

[23] D. Heck et al., Report FZKA 6019, Forschungszentrum Karlsruhe (1998).

ACCEPTED MANUSCRIPT